Machine Learning-Based Surrogate Modelling of Reflectarray Unit Cell in a 4-D Parallelotope-Shaped Domain

Daniel R. Prado, Jesús A. López-Fernández and Manuel Arrebola
Group of Signal Theory and Communications, Universidad de Oviedo, Spain. Email: {drprado, jelofer, arrebola}@uniovi.es

***Abstract*—A novel strategy to define a high-dimensionality parallelotope-shaped domain is proposed to train surrogate models of reflectarray unit cells. The concept is based on the definition of a region or rectangle of stability where sharp resonances are avoided as much as possible. Then, a 4-D parallelotope is defined around the rectangle of stability, controlling its size in order to avoid new resonances that appear as a consequence of increasing the dimensionality of the domain. This methodology is applied to generate surrogate models of a multi-resonant unit cell based on support vector regression. Results show a high degree of agreement between the obtained surrogate models and simulations based on the method of moments based on local periodicity tool that was used to generate the training samples. Furthermore, the proposed method performs better than lower dimensionality methods for wideband optimization.**

***Index Terms*—Surrogate modelling, machine learning, support vector regression, reflectarray unit cell, method of moments**

I. Introduction

The electromagnetic response of reflectarray unit cells is obtained by means of a full-wave analysis tool assuming local periodicity (LP) [1]. This tool may be implemented with different techniques, although the most common is the method of moments (MoM) [1], [2]. This approach of analysis provides a good trade-off between accuracy in the predictions of the radiation patterns and computing time when compared to a full-wave analysis of the whole antenna [3]. However, when applied to the optimization of large arrays, it is still slow [4]. Thus, it is interesting to employ other techniques to further improve computing efficiency without sacrificing accuracy.

Surrogate modelling of unit cell has already been proposed for some time using a number of machine learning techniques such as artificial neural networks [5], support vector regression (SVR) [6] or ordinary kriging [7]. However, high accuracy models rely on avoiding the appearance of sharp resonances in the training domain [8]. For low-dimensionality models, this may be easy to achieve. However, multi-resonant unit cells with several degrees of freedom (DoF), employed in advanced reflectarray optimization, produce a multitude of resonances when the dimension of the input space is increased, which may cause a severe degradation of the surrogate model accuracy.

In order to overcome the limitations of new resonances when the dimensionality of the surrogate model is increased, this work proposes the definition of a novel 4-D parallelotope[1] domain around a rectangle of stability where the surrogate models may be trained. The methodology to define such training domain is general and consists in several steps. First, the geometrical DoF of the unit cell are first reduced to two by means of scaling factors. Then, the value of the scaling factors, as well as the periodicity of the unit cell, is adjusted in such a way that the plane defined by the reduced DoF avoids sharps resonances as much as possible. Then, a rectangle of stability is chosen within this plane by limiting the range of these two DoF. Next, two new DoF are added, defining a 4-D parallelotope around the rectangle of stability. These two new DoF allow to control the size of the 4-D parallelotope in such a way as to avoid new sharp resonances that appear outside the rectangle of stability in the new extra dimensions. This methodology is applied to a multi-resonant unit cell [9], for which SVR surrogate models are obtained at several frequencies and applied to a wideband reflectarray optimization. Results show a net improvement of reflectarray performance in the whole frequency band as well as superior performance when compared to the use of low-dimensionality models.

[1] A parallelotope is the generalization in N dimensions of a parallelepiped, while an orthotope is the generalization of the rectangle in N dimensions.

II. Definition of the Parallelotope Domain

A. Unit Cell Definition and Reflectarray Specifications

Although the methodology to define the 4-D parallelotope is general and can be applied to any unit cell that provides at least four DoF, it will be exemplified with the unit cell shown in Figure 1 and studied in detail elsewhere [9]. This unit cell is comprised of two sets of four parallel and coplanar dipoles in two layers of metallization. Each set of four dipoles is used to control the phase-shift for each linear polarization by means of varying the lengths of the dipoles. Since the lengths of the dipoles constitute the design DoF, the rest of the parameters will be kept constant (substrate, dipole widths, etc.). In the following sections, results were obtained employing a substrate with $h_A = 2.363\,\text{mm}$ of thickness, $\varepsilon_{r_A} = 2.55$ and $\tan\delta_A = 0.0009$ for the bottom layer, and a substrate with $h_B = 1.5\,\text{mm}$ of thickness, $\varepsilon_{r_B} = 2.17$ and $\tan\delta_B = 0.0009$ for the top layer (see Figure 1). In addition, the width of the dipoles is 0.5 mm and the separation centre to centre between parallel dipoles is 3.9 mm.

For the practical application of the surrogate models, a large reflectarray is considered, comprised of 7052 elements in a regular grid of 86×82 elements and with a feed

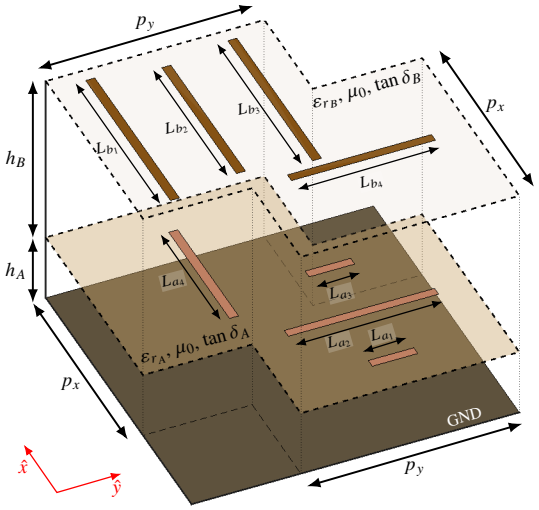

Figure 1. Sketch of the unit cell employed in this work, with several parallel and coplanar dipoles that provide several degrees of freedom.

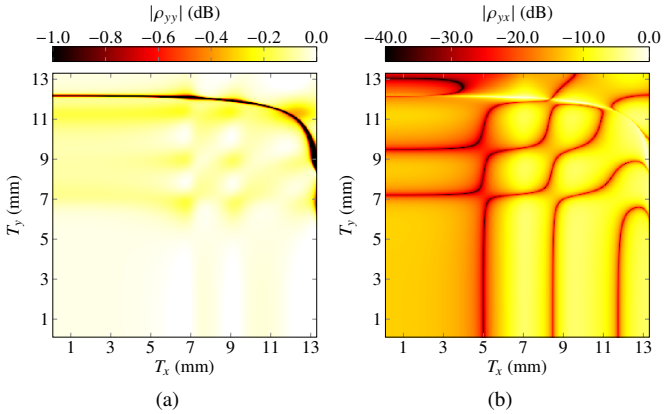

Figure 2. Magnitude of the (a) direct coefficient ρ_{yy} and (b) cross-coefficient ρ_{yx} in the (T_x, T_y) plane for oblique incidence with $(\theta = 29°, \varphi = 35°)$, a periodicity $p_x = p_y = 14\,\text{mm}$, and $\alpha_{a_1} = \alpha_{a_3} = 0.58$, $\alpha_{a_2} = \alpha_{a_4} = 1$, $\alpha_{b_1} = \alpha_{b_3} = 0.63$, $\alpha_{b_2} = 0.93$, $\alpha_{b_4} = 0.95$ at 11.85 GHz.

placed at $(-358, 0, 1070)$ mm with regard to the reflectarray center, generating an average edge illumination taper that varies between −14.8 dB and −25.3 dB in the frequency range 10.95 GHz—12.75 GHz. The antenna is placed on a satellite in geostationary orbit with a footprint providing European coverage, defined by the French national space agency CNES [10], with a minimum copolar gain requirement of 28 dBi in the coverage zone.

B. Definition of the Rectangle of Stability

The unit cell in Figure 1 provides up to eight DoF for the design and optimization of reflectarray antennas (the dipole lengths). Thus, the first step in the definition of a 4-D parallelotope is to reduced the total number of DoF from eight to two. To that end, the lengths of each set of four dipoles will be scaled with regard to one variable, T_x for the dipoles oriented in $\hat{x}$, and T_y for the dipoles oriented in $\hat{y}$:

$$\begin{aligned} &L_{a_1} = \alpha_{a_1} T_y \;;\; L_{a_2} = \alpha_{a_2} T_y \;;\; L_{a_3} = \alpha_{a_3} T_y \;;\; L_{a_4} = \alpha_{a_4} T_x \\ &L_{b_1} = \alpha_{b_1} T_x \;;\; L_{b_2} = \alpha_{b_2} T_x \;;\; L_{b_3} = \alpha_{b_3} T_x \;;\; L_{b_4} = \alpha_{b_4} T_y. \end{aligned} \tag{1}$$

The values of the scaling factors α_a and α_b should be selected such that sharp resonances are avoided as much as possible in the (T_x, T_y) plane while achieving a sufficiently large and smooth phase response of the direct reflection coefficients. In addition, it could also be interesting to enforce symmetry between the lateral dipoles (i.e., $\alpha_{a_1} = \alpha_{a_3}$ and $\alpha_{b_1} = \alpha_{b_3}$) since this helps to reduce the cross-polarization introduced by the unit cell [9]. Finally, the periodicity of the unit cell, p_x and p_y, as well as the range where T_x and T_y vary must be chosen. When choosing the unit cell periodicity, in addition to try to avoid sharp resonances, it is convenient to also avoid the appearance of grating lobes [1]. Regarding the range of variation of T_x and T_y, physical constraints must be met, such as considering only positive values, since these variables encode the length of dipoles; avoiding overlapping between adjacent dipoles; and complying with the maximum length imposed by the unit cell periodicity.

An example is shown in Figure 2, where the magnitude of reflection coefficients ρ_{yy} and ρ_{yx} is shown in a subset of the (T_x, T_y) plane for oblique incidence $(\theta = 29°, \varphi = 35°)$ at 11.85 GHz. For this case, the chosen scaling parameters are the same as the ones suggested in [9], while the periodicity is $p_x = p_y = 14\,\text{mm}$. As can be seen, a sharp resonance appears for high values of T_x and T_y that transfers energy from the direct coefficient ρ_{yy} to the cross-coefficient ρ_{yx}. However, for values of T_x and T_y lower than 11 mm an area with low ripples and no sharp resonances appears. Although not shown, the total phase-shift achieved in that area for ρ_{yy} is larger than 500°, which is suitable for reflectarray design [1]. In this way, a stability region has been found for $T_x, T_y \in [0.1, 11]$mm. The maximum value shown in Figure 2 for T_x and T_y was chosen such that adjacent dipoles do not overlap each other. If the periodicity is reduced from 14 mm to 12 mm, no sharp resonances appear in the maximum allowable subset in the (T_x, T_y) plane, and it will be used for the remaining of the paper, with $T_x, T_y \in [4, 10]$mm to limit those variables to a region where the phase-shift varies with the lengths of the dipoles [8].

C. Extending the Rectangle of Stability to a 4-D Parallelotope

The next step it to extend the model to include more geometrical DoF. In order to extend the model to four dimensions, we define the hyper-plane $(T_{x_1}, T_{x_2}, T_{y_1}, T_{y_2})$, whose variable are related to the dipole lengths of Figure 1 as follows:

$$\begin{aligned} &L_{a_1} = \alpha'_{a_1} T_{y_1} \;;\; L_{a_2} = \alpha'_{a_2} T_{y_2} \;;\; L_{a_3} = \alpha'_{a_3} T_{y_1} \;;\; L_{a_4} = \alpha'_{a_4} T_{x_2} \\ &L_{b_1} = \alpha'_{b_1} T_{x_1} \;;\; L_{b_2} = \alpha'_{b_2} T_{x_2} \;;\; L_{b_3} = \alpha'_{b_3} T_{x_1} \;;\; L_{b_4} = \alpha'_{b_4} T_{y_2}. \end{aligned} \tag{2}$$

However, when training in the whole hyper-plane, the accuracy of the obtained models is not high enough even when considerably increasing the number of training samples. Moreover, training times increase substantially due to the higher dimensionality and number of training samples, deeming this

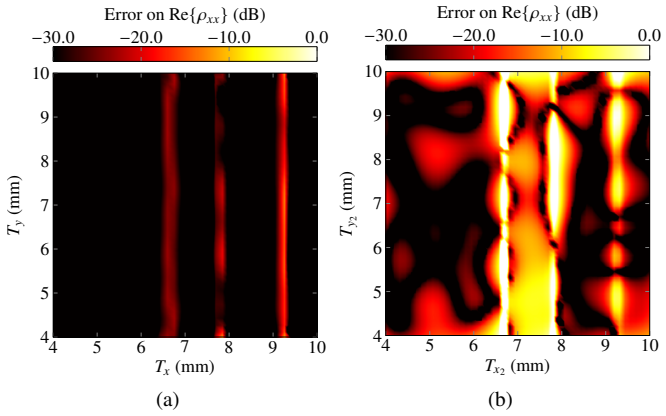

Figure 3. Relative error in dB of the real part of the estimated direct coefficient ρ_{xx} at the stability rectangle for oblique incidence with ($\theta = 29°, \varphi = 35°$) and a periodicity $p_x = p_y = 12\,\text{mm}$ when the SVR is trained using 2500 random samples placed at (a) the stability rectangle and (b) the most fitted orthotope containing the stability rectangle. The frequency is 11.85 GHz.

approach unsuitable. The loss of accuracy can be seen in Figure 3. On the one hand, Figure 3(a) shows the relative error of the SVR surrogate model for the real part of direct coefficient ρ_{xx} in the stability rectangle. The error is lower than $-30\,\text{dB}$ in most of the rectangle, with an average value of $-37.2\,\text{dB}$ in the whole rectangle. On the other hand, Figure 3(b) shows the relative error when the training domain is the fittest orthotope containing the rectangle of stability (shown in blue in Figure 4(a) and Figure 4(b)). Now, the error is close to 0 dB for a non-negligible number of considered points, and the average error in the orthotope is $-16.5\,\text{dB}$. Similar results were obtained for other reflection coefficients and angles of incidence.

To improve the accuracy of the 4-D SVR models without increasing the number of training samples, it is proposed to perform the training in a restricted domain around the rectangle of stability. To that end, we define a 4-D parallelotope with variables $(T_{x_2}, T_{y_2}, \Delta_x, \Delta_y)$ as:

$$\begin{aligned} T_{x_1} &= \alpha_{b_1} T_{x_2} \pm \Delta_x, \\ T_{y_1} &= \alpha_{a_1} T_{y_2} \pm \Delta_y. \end{aligned} \tag{3}$$

and:

$$\begin{aligned} \alpha'_{a_1} = \alpha'_{a_3} = 1 \quad ; \quad \alpha'_{a_2} = \alpha_{a_2} \quad ; \quad \alpha'_{a_4} = \alpha_{a_4} \\ \alpha'_{b_1} = \alpha'_{b_3} = 1 \quad ; \quad \alpha'_{b_2} = \alpha_{b_2} \quad ; \quad \alpha'_{b_4} = \alpha_{b_4} \end{aligned} \tag{4}$$

The two new variables Δ_x and Δ_y define, respectively, the size of the parallelotope in the T_{x_1} and T_{y_1} dimensions (see Figure 4). In this way, Δ_x and Δ_y allow to control how far from the rectangle of stability the models are trained. Please note that when $\Delta_x = \Delta_y = 0$ the model is reduced to the 2-D case of (1), with $T_{x_2} = T_x$, $T_{y_2} = T_y$, $\alpha_{a_1} = \alpha_{a_3}$ and $\alpha_{b_1} = \alpha_{b_3}$, preserving the symmetry of the lateral dipoles. Figure 4 shows a representation of different projections of the 4-D parallelotope in 2-D and 3-D subspaces, illustrating, in red color, the rectangle of stability as well.

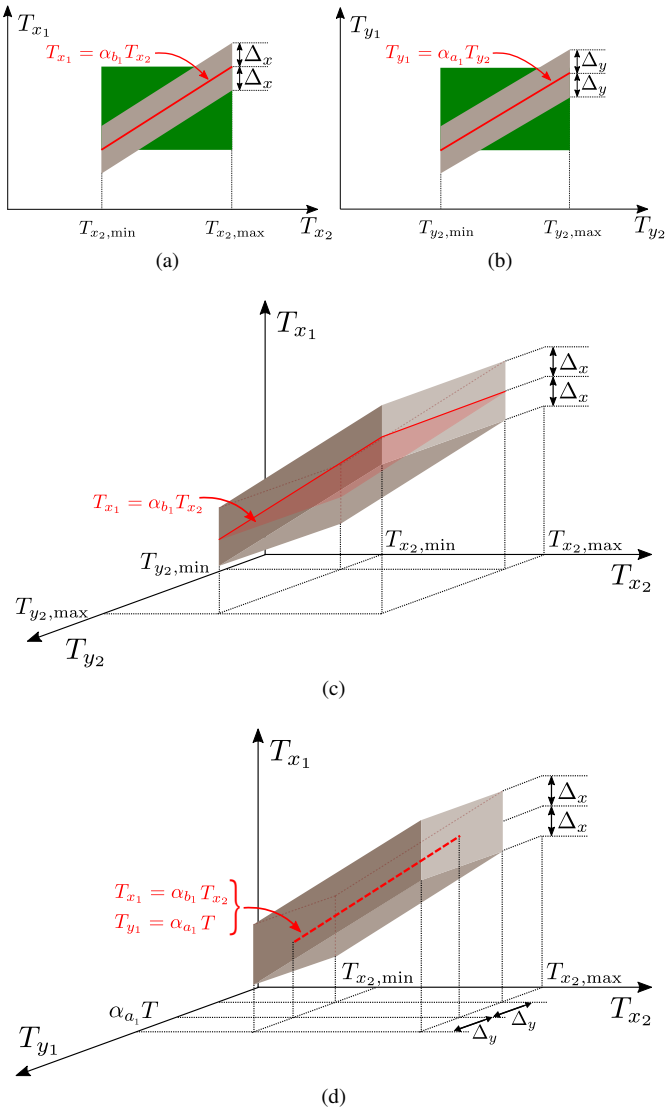

Figure 4. Low-dimensionality illustration of the region where the SVR models are trained depending on the variables from (2) (in green) and (3) (in gray). (a) Parallelogram (rectangle) yielded by the orthogonal projection of the parallelotope (orthotope) SVR domain over the (T_{x_1}, T_{x_2}) subspace. (b) Parallelogram (rectangle) produced by the orthogonal projection of the parallelotope (orthotope) SVR domain over the (T_{y_1}, T_{y_2}) subspace. (c) Parallelepiped yielded by the orthogonal projection of the parallelotope SVR domain over the $(T_{x_1}, T_{x_2}, T_{y_2})$ subspace. (d) Parallelepiped that results from the cut of the parallelotope SVR domain along the hyperplane $T_{y_2} = T$. For the sake of clarity, only the orthogonal projections of the fittest orthotope are depicted (beneath the parallelotope projections). In all cases, the stability region is plotted in red.

III. Application to Wideband Optimization

A. SVR Model Training Specifications

A set of SVR models in a 4-D parallelotope with $\Delta_x, \Delta_y \in [0, 0.5]$ mm will be trained at five equispaced frequencies in the range 10.95 GHz – 12.75 GHz in order to perform a wideband reflectarray optimization. The training process consists on an efficient grid search in the plane defined by the SVR parameters based on cross-validation. To that end,

Table I

FIGURES OF MERIT OF A EUROPE COVERAGE AFTER A WIDEBAND OPTIMIZATION AT FIVE DIFFERENT FREQUENCIES WITH A 2-D SVR ($\Delta_x = \Delta_y = 0$ mm) AND A 4-D SVR ($\Delta_x, \Delta_y \in [0, 0.5]$ mm). OPTIMIZED LAYOUTS WERE SIMULATED WITH MOM-LP. CP_{MIN} IS IN DBI AND XPI IS IN DB.

	10.95 GHz		**11.40 GHz**		**11.85 GHz**		**12.30 GHz**		**12.75 GHz**	
	CP_{min}	**XPI**	**CP_{min}**	**XPI**	**CP_{min}**	**XPI**	**CP_{min}**	**XPI**	**CP_{min}**	**XPI**
Initial layout	23.38	25.86	27.77	30.06	29.89	32.25	26.78	29.01	22.35	23.85
Opt. SVR 2D	27.30	31.95	29.07	34.86	29.36	35.79	29.06	35.70	27.93	34.47
Opt. SVR 4D	28.09	38.48	28.59	39.25	28.95	39.73	28.64	39.21	28.19	38.54

a total of 2500 random samples per angle of incidence and frequency are generated with the MoM-LP described in [2] are considered. They are divided into three disjoint sets: 1750 for training, 375 for validation and 375 for test. In addition, models are generated for 152 different angles of incidence, since the angles of incidence are not considered as input variables to the model. Then different models per angle of incidence and frequency are considered: the real and imaginary part of each reflection coefficient, plus the magnitude of the two direct coefficients. More details on the training process may be found in [6]. In addition, 2-D SVR models ($\Delta_x = \Delta_y = 0$) will also be trained in the same conditions to compare with the 4-D models.

The achieved average test error, compared with the reference MoM-LP tool, across all reflection coefficient models, angles of incidence and frequencies is -29.8 dB for the 4-D models, while it is -40.1 dB for the 2-D models, guaranteeing a high degree of accuracy for the prediction of radiation patterns [6].

B. Wideband Optimization

Table I shows the results for the dual-linear wideband optimization. For each frequency, the worst result between both linear polarizations is shown. The optimizations were carried out with the SVR models, but the shown results were obtained after simulating the initial and optimized layouts with the MoM-LP [2]. Performance of the initial layout quickly deteriorates as it is simulated further away from the design frequency (11.85 GHz). After the optimization with the 2-D SVR, both copolar and cross-polarization performances are improved across all frequencies. However, the minimum copolar gain does not comply with the goal of 28 dBi. The 4-D SVR provides extra DoF to improve the performance of the antenna. Indeed, in addition to improving the copolar gain, complying with the goal of achieving at least 28 dBi at all frequencies, cross-polarization performance is further improved, showing how the 4-D SVR provides an edge when compared to the 2-D SVR for wideband and dual-band reflectarray direct optimization.

IV. CONCLUSION

A novel methodology to train surrogate models in a 4-D parallelotope-shaped domain has been presented. It is based on defining a rectangle of stability in 2-D that is later extended to 4-D by means of auxiliary DoF. In this way, the 4-D parallelotope domain is able to avoid sharp resonances that appear as a consequence of increasing the models dimensionality. Following this methodology, a set of SVR models were trained for application in a wideband reflectarray optimization, showing superior results than their low-dimensionality counterpart.

ACKNOWLEDGMENT

This work was supported in part by the Ministerio de Ciencia, Innovación y Universidades under project IJC2018-035696-I; by MICIN/AEI/10.13039/501100011033 under project PID2020-114172RB-C21 (ENHANCE-5G); by Gobierno del Principado de Asturias under project AYUD/2021/51706.

REFERENCES

[1] J. Huang and J. A. Encinar, *Reflectarray Antennas*. Hoboken, NJ, USA: John Wiley & Sons, 2008.

[2] R. Florencio, R. R. Boix, and J. A. Encinar, "Enhanced MoM analysis of the scattering by periodic strip gratings in multilayered substrates," *IEEE Trans. Antennas Propag.*, vol. 61, no. 10, pp. 5088–5099, Oct. 2013.

[3] I. González, A. Tayebi, J. Gomez, C. Delgado, and F. Cátedra, "Fast analysis of a dual-band reflectarray using two different numerical approaches based on the moment method," *IEEE Trans. Antennas Propag.*, vol. 61, no. 4, pp. 2333–2336, Apr. 2013.

[4] D. R. Prado, M. Arrebola, M. R. Pino, and G. Goussetis, "Contoured-beam dual-band dual-linear polarized reflectarray design using a multi-objective multi-stage optimization," *IEEE Trans. Antennas Propag.*, vol. 68, no. 11, pp. 7682–7687, Nov. 2020.

[5] P. Robustillo, J. Zapata, J. A. Encinar, and J. Rubio, "ANN characterization of multi-layer reflectarray elements for contoured-beam space antennas in the Ku-band," *IEEE Trans. Antennas Propag.*, vol. 60, no. 7, pp. 3205–3214, Jul. 2012.

[6] D. R. Prado, J. A. López-Fernández, G. Barquero, M. Arrebola, and F. Las-Heras, "Fast and accurate modeling of dual-polarized reflectarray unit cells using support vector machines," *IEEE Trans. Antennas Propag.*, vol. 66, no. 3, pp. 1258–1270, Mar. 2018.

[7] M. Salucci, L. Tenuti, G. Oliveri, and A. Massa, "Efficient prediction of the EM response of reflectarray antenna elements by an advanced statistical learning method," *IEEE Trans. Antennas Propag.*, vol. 66, no. 8, pp. 3995–4007, Aug. 2018.

[8] D. R. Prado, J. A. López-Fernández, M. Arrebola, M. R. Pino, and G. Goussetis, "Wideband shaped-beam reflectarray design using support vector regression analysis," *IEEE Antennas Wireless Propag. Lett.*, vol. 18, no. 11, pp. 2287–2291, Nov. 2019.

[9] R. Florencio, J. A. Encinar, R. R. Boix, V. Losada, and G. Toso, "Reflectarray antennas for dual polarization and broadband telecom satellite applications," *IEEE Trans. Antennas Propag.*, vol. 63, no. 4, pp. 1234–1246, Apr. 2015.

[10] J. A. Encinar, M. Arrebola, M. Dejus, and C. Jouve, "Design of a 1-metre reflectarray for DBS application with 15% bandwidth," in *First European Conference on Antennas and Propagation (EuCAP)*, Nice, France, Nov. 6–10, 2006, pp. 1–5.